5-24-2012

# Measurement of the Entry-Spin Distribution Imparted to the High Excitation Continuum Region of Gadolinium Nuclei Via (*p*,*d*) and (*p*,*t*) Reactions

T. J. Ross

C. W. Beausang
*University of Richmond*, cbeausan@richmond.edu

R. O. Hughes

J. M. Allmond

C. Angell

***See next page for additional authors***



## Recommended Citation

Ross, T. J., C. W. Beausang, R. O. Hughes, J. M. Allmond, C. T. Angell, M. S. Basunia, D. L. Bleuel, J. T. Burke, R. J. Casperson, J. E. Escher, P. Fallon, R. Hatarik, J. Munson, S. Paschalis, M. Petri, L. Phair, J. J. Ressler, N. D. Scielzo, and I. J. Thompson. "Measurement of the Entry-Spin Distribution Imparted to the High Excitation Continuum Region of Gadolinium Nuclei Via (*p*,*d*) and (*p*,*t*) Reactions." *Physical Review C* 85, no. 5 (May 24, 2012): 051304: 1-51304: 5. doi:10.1103/PhysRevC.85.051304.

PHYSICAL REVIEW C **85**, 051304(R) (2012)

# Measurement of the entry-spin distribution imparted to the high excitation continuum region of gadolinium nuclei via (*p*,*d*) and (*p*,*t*) reactions

T. J. Ross,[1,2] C. W. Beausang,[1] R. O. Hughes,[1] J. M. Allmond,[3] C. T. Angell,[4,*] M. S. Basunia,[5] D. L. Bleuel,[6] J. T. Burke,[6] R. J. Casperson,[6] J. E. Escher,[6] P. Fallon,[5] R. Hatarik,[5] J. Munson,[4] S. Paschalis,[5,†] M. Petri,[5,†] L. Phair,[5] J. J. Ressler,[6] N. D. Scielzo,[6] and I. J. Thompson[6]

[1]*Department of Physics, University of Richmond, Richmond, Virginia 23173, USA*
[2]*Department of Physics, University of Surrey, Guildford, Surrey, GU2 7JL, UK*
[3]*JIHIR, Oak Ridge National Laboratory, Oak Ridge, Tennessee 37831, USA*
[4]*Department of Nuclear Engineering, University of California, Berkeley, California 94720, USA*
[5]*Nuclear Science Division, Lawrence Berkeley National Laboratory, Berkeley, California 94720, USA*
[6]*Lawrence Livermore National Laboratory, Livermore, California 94551, USA*

(Received 17 April 2012; published 24 May 2012)

Over the last several years, the surrogate reaction technique has been successfully employed to extract $(n,f)$ and $(n,\gamma)$ cross sections in the actinide region to a precision of ∼5% and ∼20%, respectively. However, attempts to apply the technique in the rare earth region have shown large (factors of 2–3) discrepancies between the directly measured $(n,\gamma)$ and extracted surrogate cross sections. One possible origin of this discrepancy lies in differences between the initial spin-parity population distribution in the neutron induced and surrogate reactions. To address this issue, the angular momentum transfer to the high excitation energy quasicontinuum region in Gd nuclei has been investigated. The $(p,d)$ and $(p,t)$ reactions on $^{154,158}$Gd at a beam energy of 25 MeV were utilized. Assuming a single dominant angular momentum transfer component, the measured angular distribution for the $(p,d)$ reactions is well reproduced by distorted-wave Born approximation (DWBA) calculations for $\Delta L = 4\,\hbar$ transfer, whereas the $(p,t)$ reactions are better characterized by $\Delta L = 5\,\hbar$. A linear combination of DWBA calculations, weighted according to a distribution of $L$ transfers (peaking around $\Delta L = 4$–$5\,\hbar$), is in excellent agreement with the experimental angular distributions.

DOI: 10.1103/PhysRevC.85.051304 PACS number(s): 24.87.+y, 24.50.+g, 24.10.Eq, 25.40.Hs

Direct measurements of compound nuclear reaction cross sections on short-lived unstable nuclei can be extremely challenging and are often impossible. In many such cases, the surrogate reaction technique [1–3] provides the only viable option for deducing cross sections. The goal of the surrogate reaction technique is to produce the same compound system in a similar entry region (excitation energy and spin distribution) as in the desired reaction with a stable beam and target combination. If the entry distributions can be matched, a measurement of the decay probabilities in the various exit channels combined with a calculation of the formation probability provides the cross section of interest [1–3]. Over the past several years benchmarking experiments have shown that surrogate reactions and, in particular, the various surrogate ratio techniques [4,5] can reproduce the known neutron induced cross sections to within a few percent (∼5%) for $(n,f)$ [6–10] and to about ∼20% for $(n,\gamma)$ reactions in the actinide region [11]. However, significant discrepancies have been observed when the same techniques are applied to $(n,\gamma)$ reactions in the mass 150 region or near closed shells [12–14]. A mismatch in the entry spin distributions between the $(n,\gamma)$ and surrogate reactions may contribute significantly to this discrepancy [typically light ion induced reactions have been used as surrogates, e.g., $(\alpha,\alpha')$, $(p,p')$, $(p,d)$, and $(p,t)$] [6–12]. The current paper presents the first measurement of the entry spin distribution in Gd nuclei populated following $(p,d)$ and $(p,t)$ reactions. It is interesting to note that these nuclei span a region known for a rapid change from vibrational to rotational character.

The experiment was carried out at the 88-in. cyclotron at Lawrence Berkeley National Laboratory where isotopically enriched targets of $^{158}$Gd and $^{154}$Gd were bombarded by a beam of 25-MeV protons. Charged-particle reaction products (protons, deuterons. and tritons) were detected using the STARS (silicon telescope array for reaction studies) $\Delta E$-$E$ telescope while coincident $\gamma$ rays were detected using the five clover Ge detectors of the LIBERACE (Livermore Berkeley array for collaborative experiments) [15]. The master trigger for the data acquisition required a charged-particle ($p$, $d$, or $t$)–$\gamma$-ray coincidence. In the course of the experiment approximately $10^6$ $(p,t\gamma)$ events (selecting the even-even $^{152,156}$Gd product nuclei) and $10^7$ $(p,d\gamma)$ events (selecting the even-odd $^{153,155}$Gd nuclei) were recorded. The present work focuses on data recorded on the $^{158}$Gd target. The beam energy and thicknesses of the Si telescopes in the STARS spectrometer were such that excitation energies of up to ∼10 MeV in the final nuclei could be selected by a suitable gate on the energy of the outgoing direct reaction particle (low excitation energies in the residual nuclei correspond to high particle energies and vice versa). For additional details of the experimental setup see Refs. [15–17]. Of particular relevance to this work, the angular coverage of the segmented Si detectors spanned the

[*]Current address: Quantum Beam Science Directorate, Japan Atomic Energy Agency, Tokai, Ibaraki 319-1195, Japan.
[†]Current address: IKP, TU Darmstadt, 64289 Darmstadt, Germany.

 

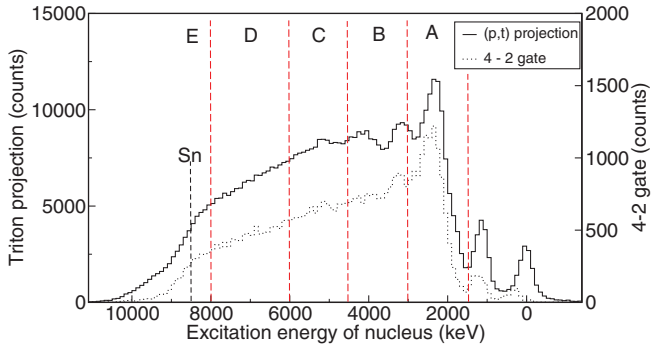


FIG. 1. (Color online) $^{158}$Gd$(p,t)$ spectrum observed in coincidence with $\gamma$ rays, solid black line. Particle energy is displayed as a function of excitation energy in the resultant $^{156}$Gd compound nucleus. The dotted line shows tritons observed in coincidence with the $4^+ \rightarrow 2^+$ yrast band transition, thus selecting all initial entry states which decay via the $4^+$ state. Five excitation energy bins (labelled A–E) which are used in the continuum region angular distribution analysis are shown.

range 33° to 53°, sufficient for a limited angular distribution measurement.

The triton and deuteron spectra following the $^{158}$Gd + $p$ reaction are shown in Figs. 1 and 2, respectively. It is important to note that these spectra directly reflect the initial entry states in $^{156}$Gd and $^{157}$Gd, i.e., states directly populated by the $(p,t)$ and $(p,d)$ reactions which subsequently decay to lower lying states by $\gamma$-ray emission. For excitation energies below the neutron separation energy, $\gamma$ decay is the only available decay mode, and therefore these spectra reflect the initial entry points into the nucleus. Also shown in Fig. 1 is the triton spectrum in coincidence with the $4^+ \rightarrow 2^+$ yrast band transition in $^{156}$Gd. In this case the $\gamma$-ray gate selects the ensemble of initial states which eventually decay through the $4^+$ level.

At low excitation energies, less than ∼1.5 MeV, the triton spectrum in Fig. 1 is dominated by a few (mainly unresolved) discrete peaks corresponding to direct population of specific low-lying levels in the nucleus. At an excitation

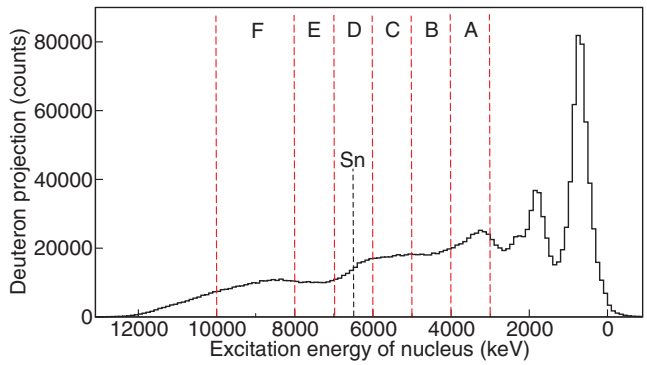


FIG. 2. (Color online) Deuteron energy spectrum from the projection of the deuteron-$\gamma$ coincidence matrix is shown in black. Particle energy is displayed as a function of excitation energy in the resultant $^{157}$Gd compound nucleus. The six excitation energy bins (labelled A–F) which are used in the continuum region angular distribution analysis are shown.

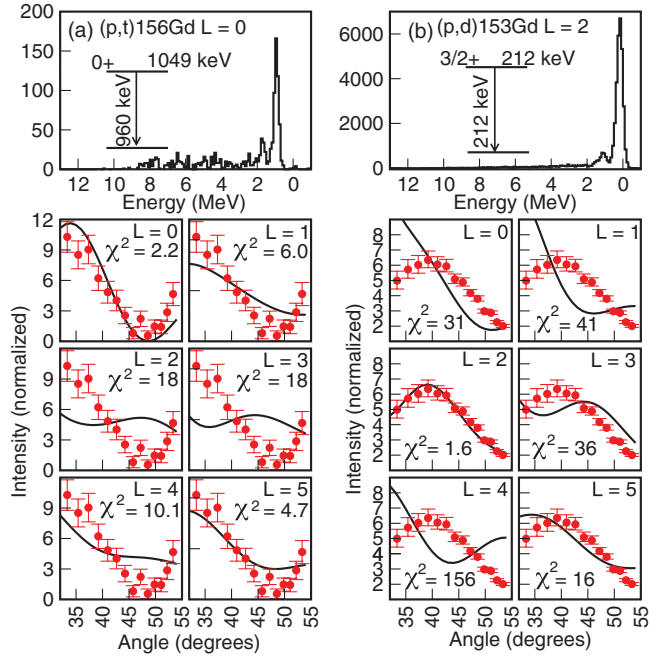


FIG. 3. (Color online) Comparison of measured and calculated (DWBA) angular distributions. (a) The distribution of tritons which directly populate the first excited $0^+$ state in $^{156}$Gd is well characterized by $\Delta L = 0\,\hbar$. (b) The distribution of deuterons which directly populate the $\frac{3}{2}^+\frac{3}{2}^+[402]$ state in $^{153}$Gd is well characterized by $\Delta L = 2\,\hbar$. See text.

energy of ∼2 MeV there is a large increase in triton intensity with a prominent peak-like feature corresponding to strong population of numerous states just above the pair gap. At higher excitation energies there is a smooth, almost linear, decrease in triton intensity up to the highest excitation energies measured in the current experiment, $E^* \sim 10$ MeV. Similar features appear in the deuteron spectrum (populating the $^{157}$Gd nucleus), Fig. 2.

Requiring a coincidence with a discrete $\gamma$-ray transition reveals the distribution of entry states that subsequently decay through the level selected by the $\gamma$-ray transition. For example, Fig. 3(a) shows the triton spectrum in coincidence with the 960 keV transition which depopulates the first excited $0^+$ level at $E^* = 1049$ keV in $^{156}$Gd. The spectrum is dominated by a single triton peak at an excitation energy corresponding to direct population of the 1049 keV level. A second smaller peak at ∼1800 keV corresponds to a second state which is also populated directly and decays through the 1049 keV state. The measured angular distribution of tritons which directly populate the 1049 keV level (i.e., those in coincidence with both the 960 keV $\gamma$ ray and the discrete triton peak at $E^* = 1049$ keV in Fig. 3(a) is shown below. The measured distribution is compared with calculated distorted-wave Born approximation (DWBA) angular distributions for various angular momentum transfer values from $\Delta L = 0$–$5\hbar$. The data are clearly best reproduced by a $\Delta L = 0\hbar$ transfer as expected for this $0^+$ state. A reduced chi-squared measurement of best fit confirms that the data are best fit by the $\Delta L = 0$ calculation. It is worth emphasizing that the curves are not fits to the

TABLE I. Optical model parameters used in calculating the $(p,d)$ and $(p,t)$ angular distributions. These parameters were obtained from Refs. [19–22]. Notation used is in accordance with the notation of Ref. [23].

| Reaction/ Particle | $V_{SO}$ | $r_{SO}$ | $a_{SO}$ | $V$ | $r_0$ | $a_0$ | $W$ | $R_W$ | $a_W$ | $W_d$ | $R_d$ | $a_d$ | Ref. |
|---|---|---|---|---|---|---|---|---|---|---|---|---|---|
| $(p,d)/p$ | 12.0 | 1.10 | 0.70 | 55.7 | 1.20 | 0.70 | – | – | – | 11.3 | 1.25 | 0.70 | Fleming *et al.* [19] param. set D |
| $(p,d)/d$ | – | – | – | 100.7 | 1.15 | 0.81 | – | – | – | 18.9 | 1.34 | 0.68 | Perey and Perey [20] param. set B |
| $(p,t)/p$ | 6.2 | 1.01 | 0.75 | 55 | 1.17 | 0.75 | 2.8 | 1.32 | 0.64 | 7.82 | 1.32 | 0.64 | Becchetti and Greenlees [21] |
| $(p,t)/t$ | 2.5 | 1.20 | 0.72 | 159.7 | 1.2 | 0.72 | 18.00 | 1.4 | 0.84 | – | – | – | Becchetti and Greenlees [22] |

data. Rather, for all comparisons of angular distribution data, the calculated and measured distributions are normalized to 100 units.

As another example, Fig. 3(b) shows the deuteron spectrum selected by a $\gamma$-ray coincidence gate on the 212 keV transition depopulating the 212 keV $\frac{3}{2}^+\frac{3}{2}^+[402]$ state in $^{153}$Gd. Again the spectrum is dominated by a single peak corresponding to direct population of the $\frac{3}{2}^+$ state. The angular distribution of these deuterons (i.e., those in coincidence with the 212 keV $\gamma$-ray transition and the discrete deuteron peak at $E^* = 212$ keV) is shown at the bottom of Fig. 3(b). As expected, the data are best reproduced by $\Delta L = 2\,\hbar$ transfer. Similar results are obtained for other states directly populated by the $(p,d)$ and $(p,t)$ reactions. In general, within the statistical uncertainty, the measured angular distribution is well reproduced by the known $L$ transfer to the state of interest for discrete states. It should be noted that in the limited angular range subtended by the Si detectors, some calculated curves are quite similar and cannot be distinguished by the data.

The DWBA angular distribution calculations were carried out with DWUCK4 [18] using the optical model parameters summarized in Table I. The parameters used were chosen because they most accurately reproduce the experimental angular distributions for directly populated states at low excitation energies in $^{152,153,156,157}$Gd (see, e.g., Fig. 3). The orbitals used to determine the number of di-neutron oscillator quanta in the $(p,d)$ and $(p,t)$ calculations are summarized in Table II.

In the following analysis, where the higher excitation energy quasicontinuum region is studied, the same parameters were used; however, the $Q$ value was adjusted to account for the higher excitation energy. This adjustment is responsible for the different calculated curves in Figs. 5 and 6.

Having established the sensitivity of the angular distributions to the $L$-transfer for discrete states we move on to investigate the properties of the quasicontinuum. For this analysis, several wide energy bins in the quasicontinuum region were employed, shown in Figs. 1 and 2 for the $(p,t)$ and $(p,d)$ analyses, respectively.

For the $^{158}$Gd$(p,d)^{157}$Gd reaction, the angular distributions of the deuterons for each different continuum excitation energy bin (no $\gamma$-ray coincidence required) is shown in the top row of Fig. 4. The distribution tends to become more uniform with increasing excitation energies. A similar plot for the $(p,t)$ reaction is shown in the second row of Fig. 4. As for the $(p,d)$ reaction, the angular distribution of the tritons tends to flatten with increasing excitation energies. As we will see, this flattening corresponds to a higher average angular momentum transfer at higher excitation energies.

This can be inferred from the angular distribution of tritons in the 3–6 MeV excitation energy range (bins B and C) when selected by a coincidence with the $2^+ \rightarrow 0^+$, $4^+ \rightarrow 2^+$, $6^+ \rightarrow 4^+$, and $8^+ \rightarrow 6^+$ transitions in the yrast band of $^{156}$Gd, bottom row of Fig. 4. The $\gamma$-ray coincidence selects initial entry populations which subsequently decay via the level selected by the gate. The angular distribution becomes more uniform with the increasing spin of the state selected.

It should be noted that in Fig. 4, the highest energy bin in the triton spectrum is above the neutron separation energy. Therefore, data for this bin were also selected by a coincidence requirement with an intense yrast band $\gamma$-ray transition in $^{156}$Gd (the 344 keV $4^+ \rightarrow 2^+$ transition). Although the two highest energy bins in the deuteron data are also above the separation energy for $^{157}$Gd, such a $\gamma$-ray coincidence is not feasible because of the highly fragmented $\gamma$-ray cascade in the odd nucleus and because neutron emission rapidly dominates over $\gamma$ decay for these excitation energies.

The angular distribution of deuterons in the 5–6 MeV excitation energy range (energy bin C) is compared to calculated DWBA angular distributions (adjusted for $E^* \sim 5$ MeV) for different angular momentum transfers from $\Delta L = 0$ to $\Delta L = 6\,\hbar$ in Fig. 5. A reduced chi-squared analysis is used to compare the experimental distribution to each of the calculated curves. Assuming a single $L$-transfer value, the deuteron distribution is best reproduced by $\Delta L = 4\,\hbar$ ($\chi^2 = 0.49$).

Similarly the angular distribution of tritons in the 3–6 MeV excitation energy range (energy bins B + C) are compared to

TABLE II. Occupied orbitals used to determine the number of di-neutron oscillator quanta in the DWBA calculations.

| $\Delta L$ ($\hbar$) | 0 | 1 | 2 | 3 | 4 | 5 | 6 |
|---|---|---|---|---|---|---|---|
| $(p,d)$ | $3s\frac{1}{2}$ | $2f\frac{7}{2}$ | $2d\frac{3}{2}$ | $2f\frac{7}{2}$ | $2d\frac{5}{2}$ | $3h\frac{11}{2}$ | $1g\frac{7}{2}$ |
| $(p,t)$ | $1g\frac{7}{2}$ | $2d\frac{5}{2}, 2f\frac{7}{2}$ | $1g\frac{7}{2}$ | $2d\frac{5}{2}, 2f\frac{7}{2}$ | $1g\frac{7}{2}$ | $2d\frac{5}{2}, 2f\frac{7}{2}$ | $1g\frac{7}{2}$ |

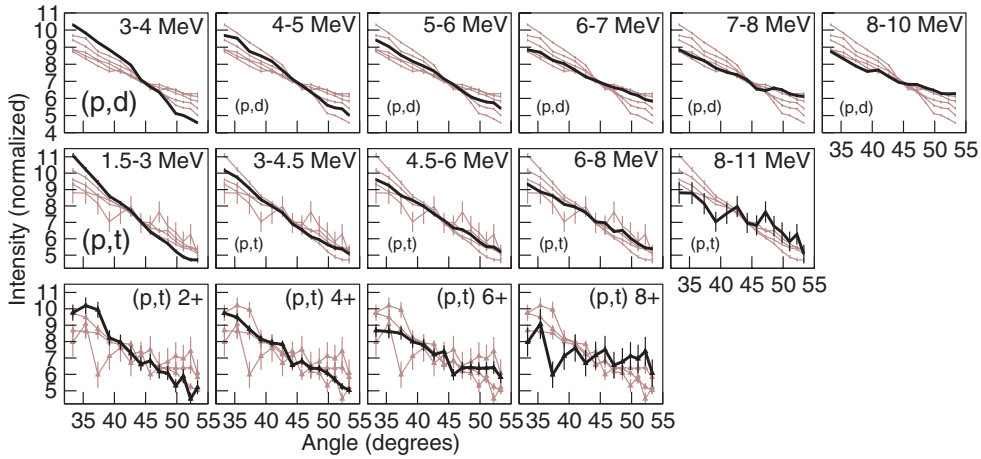


FIG. 4. (Color online) Top row: Angular distribution of outgoing deuterons [following the $^{158}$Gd$(p,d)^{157}$Gd reaction] as a function of excitation energy in $^{157}$Gd. The energy bins defined in Fig. 2 are used. The angular distribution of each energy range is shown in black (bold) and compared with each of the other energy bins. Middle row: Angular distribution of tritons [following the $^{158}$Gd$(p,t)^{156}$Gd reaction] as a function of excitation energy in $^{156}$Gd. The energy bins defined in Fig. 1 are used. Bottom row: Angular distribution of tritons in the 3–6 MeV excitation energy region (bins B and C) gated by the first four yrast band transitions in $^{156}$Gd.

calculated DWBA angular distributions for different angular momentum transfers from $\Delta L = 0$ to $\Delta L = 6\,\hbar$ in Fig. 6. Assuming a single $L$-transfer value, the experimental distribution is best reproduced by $\Delta L = 5\,\hbar$ ($\chi^2 = 11$).

Of course, the spin transfer into the continuum is not expected to be of single integer value but rather a distribution, probably peaking around a specific spin value. Indeed Escher *et al.* [24] have been able to model this distribution for the $^{158}$Gd$(p,t)^{156}$Gd reaction. By modeling the decay of $^{156}$Gd with a modified Hauser-Feshbach calculation for many different spin-parity distributions, and comparing the calculated relative yrast band $\gamma$-ray intensities with the measured intensities from this experiment, the most likely spin-parity distribution was found. The distribution peaks around 4–5 $\hbar$ with smaller contributions from lower spin transfer values. Considering spin-transfer values of $\Delta L = 0$ through 6 $\hbar$, the distribution of Escher *et al.* is shown in Table III. Using these values a weighted sum of the individual DWBA curves excellently reproduces the experimental angular distributions of tritons following the $^{158}$Gd$(p,t)^{156}$Gd reaction as shown in Fig. 6.

Examination of the intensity flow through the low-lying level schemes of the even-even Gd nuclei reveals that $\Delta L =$ 4–5 $\hbar$ transfer is quite reasonable. For $^{156}$Gd, the $2^+$ level is fed only through known discrete low-lying levels, mainly from the $4^+$ yrast band level (80% of the intensity) and a variety of nonyrast $0^+$, $2^+$ discrete states around 1 MeV excitation energy. There is very little ($\sim$ none) direct side-feeding from higher lying quasicontinuum states. Therefore, the initial entry states must first decay through these lower lying states. Since most of the $2^+$ intensity comes via the $4^+$ level, an initial entry spin centered around $\Delta L = 4$–5 $\hbar$ is not unreasonable. This result is also similar to the results of Guttormsen *et al.*

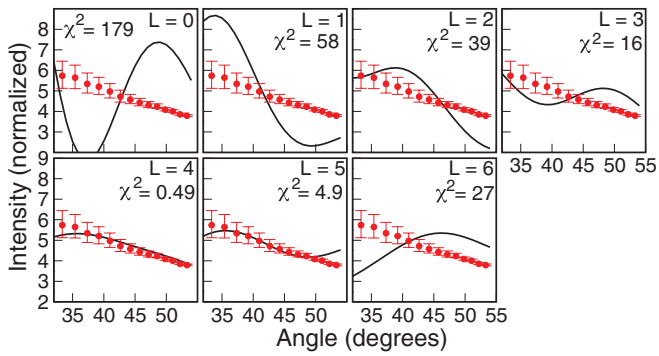


FIG. 5. (Color online) Angular distribution of the deuterons following the $^{158}$Gd$(p,d)^{157}$Gd reaction which correspond to direct population of the quasicontinuum region in $^{157}$Gd (5–6 MeV) is shown compared with the calculated DWBA angular distributions.

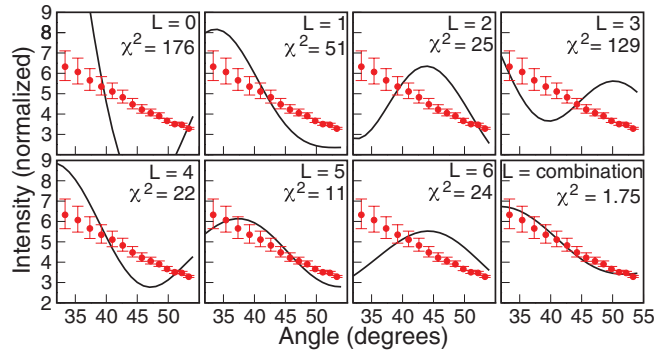


FIG. 6. (Color online) The angular distribution of the tritons following the $^{158}$Gd$(p,t)^{156}$Gd reaction which correspond to direct population of the quasicontinuum region in $^{156}$Gd (4.5–6 MeV) is shown compared with the calculated DWBA angular distributions. The experimental data are also compared with a weighted combination of the DWBA curves.

TABLE III. The distribution of Escher *et al*. [24] based upon side feeding of the yrast band in $^{156}$Gd.

| $\Delta L$ ($\hbar$) | 0 | 1 | 2 | 3 | 4 | 5 | 6 |
|---|---|---|---|---|---|---|---|
| | 2% | 6% | 6% | 8% | 31% | 41% | 6% |

[25] who measured an angular momentum transfer of $\sim 5\ \hbar$ when populating dysprosium nuclei via the ($^3$He,$\alpha$) reaction mechanism.

A transferred spin distribution peaking at $\Delta L \sim 4$–$5\ \hbar$ is significantly higher than one would expect of an $(n,\gamma)$ reaction. In a study of Gd nuclei by the $(p,p')$ mechanism, Scielzo *et al*. [12] carry out calculations which suggest that the $(n,\gamma)$ reaction populates the compound nucleus with a spin distribution which peaks around $\Delta L = 1$–$2\ \hbar$. This mismatch may be responsible for discrepancies in cross-section measurements when utilizing light ion reactions as surrogates for neutron induced reactions.

In conclusion, the combination of particle angular distributions and coincident $\gamma$-ray detection has been demonstrated as a powerful tool for measuring both the spin of directly populated discrete states and the spin input to the quasicontinuum following light-ion transfer reactions. The very high selectivity of this technique could prove invaluable as attention turns to the study of exotic rare isotopes where statistics are limited. The entry spin distribution imparted to the highly excited quasicontinuum in Gd nuclei, between ~2 and 10 MeV, has been measured for $(p,d)$ and $(p,t)$ reactions at $E_{\text{beam}} = 25$ MeV. For the $(p,d)$ reaction, the experimental angular distribution was most clearly reproduced by $\Delta L = 4\ \hbar$ transfer. Similarly, the entry spin imparted into $^{156}$Gd by $(p,t)$ reactions was measured and found to most closely resemble an angular momentum transfer of $\Delta L = 5\ \hbar$. A linear combination of DWBA curves according to the spin distribution of Escher *et al*. [24] is in excellent agreement with the experimental distribution for the $(p,t)$ reaction.

The authors thank the 88-in. cyclotron operations and facilities staff for their help in performing this experiment. This work was performed under the auspices of the National Science Foundation and the US Department of Energy by the University of Richmond under Grant Nos. DE-FG52-06NA26206 and DE-FG02-05ER41379, Lawrence Livermore National Laboratory under Contracts No. W-7405-Eng-48 and No. DE-AC52-07NA27344, and Lawrence Berkeley National Laboratory under Contract No. DE-AC02-05CH11231.

[1] J. D. Cramer and H. C. Britt, Nucl. Sci. Eng. **41**, 177 (1970).
[2] J. D. Cramer and H. C. Britt, Phys. Rev. C **2**, 2350 (1970).
[3] J. E. Escher, J. T. Burke, F. S. Dietrich, N. D. Scielzo, I. J. Thompson, and W. Younes, Rev. Mod. Phys. **84**, 353 (2012).
[4] C. Plettner *et al*., Phys. Rev. C **71**, 051602(R) (2005).
[5] J. E. Escher and F. S. Dietrich, Phys. Rev. C **74**, 054601 (2006).
[6] J. J. Ressler *et al*., Phys. Rev. C **83**, 054610 (2011).
[7] S. R. Lesher *et al*., Phys. Rev. C **79**, 044609 (2009).
[8] J. T. Burke *et al*., Phys. Rev. C **73**, 054604 (2006).
[9] R. O. Hughes *et al*., Phys. Rev. C **85**, 024613 (2012).
[10] G. Kessedjian *et al*., Phys. Lett. B **692**, 297 (2010).
[11] J. M. Allmond *et al*., Phys. Rev. C **79**, 054610 (2009).
[12] N. D. Scielzo *et al*., Phys. Rev. C **81**, 034608 (2010).
[13] J. E. Escher and F. S. Dietrich, Phys. Rev. C **81**, 024612 (2010).
[14] C. Forssén, F. S. Dietrich, J. Escher, R. D. Hoffman, and K. Kelley, Phys. Rev. C **75**, 055807 (2007).
[15] S. R. Lesher *et al*., Nucl. Instrum. Methods A **621**, 286 (2010).
[16] T. J. Ross *et al*. (unpublished).
[17] J. M. Allmond *et al*., Phys. Rev. C **81**, 064316 (2010).
[18] P. D. Kunz, DWUCK4, University of Colorado (unpublished).
[19] D. G. Fleming, M. Blann, H. W. Fulbright, and J. A. Robbins, Nucl. Phys. A **157**, 1 (1970).
[20] C. M. Perey and F. G. Perey, Phys. Rev. **132**, 755 (1963).
[21] F. D. Becchetti Jr. and G. W. Greenlees, Phys. Rev. **182**, 1190 (1969).
[22] F. D. Becchetti Jr. and G. W. Greenlees, in *Polarization Phenomena in Nuclear Reactions*, edited by H. H. Barschall and W. Haeberli (University of Wisconsin, Madison, WI, 1971), p. 682.
[23] C. M. Perey and F. G. Perey, At. Data Nucl. Data Tables **17**, 1 (1976).
[24] J. E. Escher *et al*. (unpublished).
[25] M. Guttormsen, L. Bergholt, F. Ingebretsen, G. Løvhøiden, S. Messelt, J. Rekstad, T. S. Tveter, H. Helstrup, and T. F. Thorsteinsen, Nucl. Phys. A **573**, 130 (1994).